Available online at www.sciencedirect.com
SCIENCE DIRECT®
Journal of Solid State Chemistry 179 (2006) 2721–2727
JOURNAL OF SOLID STATE CHEMISTRY
www.elsevier.com/locate/jssc

Thermodynamic properties of complex oxides in the La–Ni–O system

D.O. Bannikov*, V.A. Cherepanov

Ural State University, Lenin av 51, Ekaterinburg 620083, Russia

Received 13 April 2006; received in revised form 24 May 2006; accepted 25 May 2006
Available online 2 June 2006

Abstract

Complex oxides $La_2NiO_{4+\delta}$, $La_3Ni_2O_{7-\delta}$, $La_4Ni_3O_{10-\delta}$ and $LaNiO_{3-\delta}$, the members of Ruddlesden–Popper series $La_{n+1}Ni_nO_{3n+1}$, were prepared using citrate precursors. The stability range of $LaNiO_{3-\delta}$ in air as well as the oxygen nonstoichiometry of $La_3Ni_2O_{7-\delta}$ and $La_4Ni_3O_{10-\delta}$ as a function of temperature and oxygen partial pressure was determined by means of thermogravimetric technique. Decomposition temperatures of $La_3Ni_2O_{7-\delta}$, $La_4Ni_3O_{10-\delta}$ and $LaNiO_{3-\delta}$ in air were determined by conductivity measurement method. The boundary of stability for $La_4Ni_3O_{10-\delta}$ was determined by EMF measurements of galvanic cell with oxygen conducting solid electrolyte. The isothermal (1400 K) projection of La–Ni–O system phase diagram to the plane "log(PO_2)–relative mole fraction of metal components" was suggested.

Keywords: Lanthanum nickelates; Thermodynamic stability; Phase diagram; Oxygen nonstoichiometry

1. Introduction

The structure of lanthanum nickelates with general formula $La_{n+1}Ni_nO_{3n+1}$ is similar to those of the Ruddlesden–Popper series. In these nickelates, n consecutive perovskite layers $(LaNiO_3)_n$ alternate with rock salt (RS) layers (LaO) along the crystallographic c direction, so their formula can be represented as $(LaO)(LaNiO_3)_n$. Four complex oxides belonging to this homologous series: La_2NiO_4 ($n=1$), $La_3Ni_2O_7$ ($n=2$), $La_4Ni_3O_{10}$ ($n=3$) and $LaNiO_3$ ($n=\infty$) were described in the La–Ni–O system.

$La_2NiO_{4+\delta}$ possesses either tetragonal [1–6] or orthorhombically distorted [7–11] K_2NiF_4-type crystal structure. The type of crystal structure depends on the temperature and oxygen content. It was shown that oxygen nonstoichiometry in $La_2NiO_{4+\delta}$ could widely be varied and reach values up to $\delta=0.25$ [9–11]. The equilibrium oxygen hyperstoichiometry in air is close to 0.14–0.15 at 300 K and decreases while heating [12–14].

X-ray diffraction pattern of $La_3Ni_2O_7$ allowed describing it in an orthorhombic structure in either *Fmmm* [15–17] or *Cmcm* [7,18,19] space group. Same discrepancy appears in the description of crystal structure of $La_4Ni_3O_{10}$. Orthorhombic symmetry of $La_4Ni_3O_{10}$ unit cell described within *Fmmm* space group [20,21], or lower symmetry *Cmca* space group [7,18,19]. Both phases can possess oxygen nonstoichiometry to some extent. $La_3Ni_2O_{7-\delta}$ synthesized in air at approximately same temperatures [16,18,22] is reported to have slight oxygen deficiency $\delta\approx0.08$ [16], meanwhile in [18], Rietveld refinement resulted in formula $La_3Ni_2O_{7.02}$ and chemical analysis made in [22] led to $La_3Ni_2O_{6.72}$. Oxygen content in the phase with $n=3$ reported either close to stoichiometric $La_4Ni_3O_{10}$ [21] or $La_4Ni_3O_{10.03}$ [18], or oxygen-deficient $La_4Ni_3O_{9.66}$ [22].

$LaNiO_{3-\delta}$ crystallized in the rhombohedrally distorted perovskite-type structure [23–26].

The representation of phase equilibria and thermodynamic properties of the ternary oxides in the La–Ni–O system were contradictory and changed as new data about existed phases appeared [5,6,11,25–30]. The available literature information on the thermodynamic properties and phase equilibria for the La–Ni–O system had been

*Corresponding author. Fax: +73432615978.
E-mail address: Dmitry.Bannikov@usu.ru (D.O. Bannikov).

0022-4596/$ - see front matter © 2006 Elsevier Inc. All rights reserved.
doi:10.1016/j.jssc.2006.05.026

systematically analyzed recently by Zinkevich and Aldinger [31]. Decomposition scheme, previously suggested in [15,29,30], written as

$$LaNiO_3 \rightarrow La_{n+1}Ni_nO_{3n+1} + NiO + O_2 \quad (1)$$

was detailed based on the results from the different sources. The limiting oxygen partial pressure in the row $LaNiO_3$–$La_4Ni_3O_{10}$–$La_3Ni_2O_7$–La_2NiO_4, similarly to previously studied lanthanum cobaltites [32], decreases. Decomposition reactions were presented as follows:

$$4LaNiO_3 \rightarrow La_4Ni_3O_{10} + NiO + 12O_2, \quad (2)$$

$$3La_4Ni_3O_{10} \rightarrow 4La_3Ni_2O_7 + NiO + 1/2O_2, \quad (3)$$

$$2La_3Ni_2O_7 \rightarrow 3La_2NiO_4 + NiO + 1/2O_2, \quad (4)$$

$$La_2NiO_4 \rightarrow La_2O_3 + Ni + 1/2O_2. \quad (5)$$

The literature survey shows that existed experimental information about phase relations and oxygen nonstoichiometry, especially concerning $La_3Ni_2O_{7-\delta}$ and $La_4Ni_3O_{10-\delta}$, is very less or contradictory. Therefore, the aim of the work includes systematical investigation of phase relations in the La–Ni–O system and oxygen nonstoichiometry of lanthanum nickelates.

2. Experimental

Lanthanum oxide La_2O_3 of "LaO-D" purity grade and nickel oxide NiO of "special purity" grade used as starting materials were preliminary annealed in air: La_2O_3 at 1100 °C for 12 h and NiO at 800 °C for 4 h. After that, lanthanum oxide was quickly cooled in a desiccator and then weighted. The weight of NiO was calculated according to the known amount of La_2O_3 with respect to the required composition of complex oxide.

Complex oxides La_2NiO_4, $La_3Ni_2O_7$, $La_4Ni_3O_{10}$ and $LaNiO_3$ were synthesized using the citrate route. Stoichiometric amounts of NiO and La_2O_3 were dissolved in a slight excess of diluted nitric acid solution (1/3 HNO_3, 2/3 H_2O) followed by the addition of an equivalent molar proportion of citric acid dehydrate $C_6H_8O_7 \cdot 2H_2O$ with respect to NiO and La_2O_3 in order to transform nitrates to citrates. The solution was heated to dryness and the formation of a green gel was observed during this thermal treatment. This gel was fired to dryness and the resulting citrates were slowly decomposed on a hot plate. The dark gray products were ground and heated in air at 300 °C for 3 h then at 500 °C for 3 h and finally at 800 °C for 12 h. The black powders were annealed in air in order to obtain La_2NiO_4, $La_3Ni_2O_7$, $La_4Ni_3O_{10}$ at 1100 °C and $LaNiO_3$ at 800 °C. Single-phase materials were obtained after 5 days heating followed by intermediate grindings. The samples were characterized by X-ray powder diffraction.

Thermogravimetric measurements were performed in the thermobalances as a function of oxygen partial pressure and temperature. Oxygen partial pressure was adjusted with the help of YSZ oxygen sensor. The powder sample of $LaNiO_{3-\delta}$ was dried at 850 °C for 24 h prior to use.

The samples for conductivity measurement were pressed in the form of bars under pressure of 7×10^9 Pa with addition of small amount of 10% polyvinyl alcohol solution. The bars of $La_3Ni_2O_7$, $La_4Ni_3O_{10}$ and La_2NiO_4 were slowly heated and sintered at 1100 °C during 24 h. Sintering temperature of $LaNiO_3$ was 800 °C during 24 h. Since the conductivity data were used only for thermodynamic analysis, the density of sintered samples was not determined. Temperature dependences of electrical conductivity were measured by 4-probe method in air. An isothermal region inside the furnace has been determined before the experiment to exclude thermoelectrical effect influence.

Thermodynamic stability limits of complex oxides were determined by EMF measurements of galvanic cell with oxygen conducting solid electrolyte. The feature of the setup used was the possibility for changing of oxygen partial pressure on the reference electrode of the working cell in order to hold approximately same value of oxygen partial pressure at the working and reference electrodes. These prevent non-electrochemical leakage of oxygen through micropores of the ceramic into the cell, which are able to affect the equilibrium oxygen pressure. The scheme of the EMF cell used in this work was presented in [33]. Powder samples of $La_4Ni_3O_{10}$ and $La_3Ni_2O_7$ were placed into sealed cells. First cell with $La_4Ni_3O_{10}$ inside (cell 1) was heated up to 1120 °C and second cell with $La_3Ni_2O_7$ inside (cell 2) was heated up to 1100 °C. Since temperature reached a constant value, oxygen partial pressure inside the cell was adjusted electrochemically by pumping of oxygen out the cell using a solid electrolyte. Oxygen was removed from the cell by small amounts applying dc voltage (direct current ~1 mA) to the solid electrolyte. While oxygen was removed step by step, EMF of the cell increased with respect to air ($PO_2 = 0.21$ atm). However, starting with ~17.5 mV for $La_4Ni_3O_{10}$ ($T = 1120$ °C) and ~30.2 mV for $La_3Ni_2O_7$ ($T = 1100$ °C), EMF stopped changing in spite of oxygen had been still removing. It should be noticed that the time while EMF reached its constant value after polarization was very long (~40 h). Since oxygen partial pressure had become constant, it was taken as an equilibrium value. Assuming that decomposition reaction of complex oxide placed in the cell had started, we tried to measure temperature dependence of EMF (equilibrium partial pressure inside the cell). Temperature was increased by 10–15 °C and EMF was measured again until a constant value (new equilibrium value of oxygen partial pressure under the sample).

Oxygen nonstoichiometry of $La_3Ni_2O_{7-\delta}$ and $La_4Ni_3O_{10-\delta}$ was studied by TG measurements within the temperature range 900–1150 °C in air and at 1100 °C versus oxygen pressure $-1 \leqslant \log(PO_2/\text{atm}) \leqslant 0$. Unchangeable mass of the sample during approximately 2 h was supposed as equilibrium at certain conditions (T, PO_2). Equilibrium was also confirmed by the reproducibility of measured

mass when coming to a certain point from higher or lower temperature and from higher or lower PO_2. Absolute values of oxygen nonstoichiometry were determined by direct reduction of samples in the hydrogen flow in thermobalances at 1100 °C. X-ray powder diffraction of the samples after reduction procedure confirms that only La_2O_3 and Ni were presented as the products. Neither initial substances nor La_2NiO_4 or NiO were detected. Therefore, we concluded that $La_3Ni_2O_{7-\delta}$ or $La_4Ni_3O_{10-\delta}$ was completely reduced.

X-ray powder diffraction measurements were performed at DRF-4.0 and DRON-UM1 diffractometers using Cu $K\alpha$ radiation.

3. Results and discussion

3.1. Determination of decomposition temperature for $LaNiO_3$ by TGA

Temperature dependence of $LaNiO_{3-\delta}$ relative mass changes in air is shown in Fig. 1. It is easy to see that at ~980 °C, weight of the sample sharply decreased. We suggested that this sharp decrease of weight resulted by the decomposition reaction. Decomposition temperature 980 °C is in a good agreement with those obtained in [2,25]. In order to accelerate decomposition reaction, the temperature was raised up to 1050 °C. X-ray powder diffraction analysis of the rapidly cooled sample shows coexistence of $LaNiO_{3-\delta}$, $La_4Ni_3O_{10-\delta}$ and NiO after thermogravimetric measurements. This confirms that decomposition of $LaNiO_{3-\delta}$ can be represented (oxygen nonstoichiometry has not been taken into account) by reaction (2).

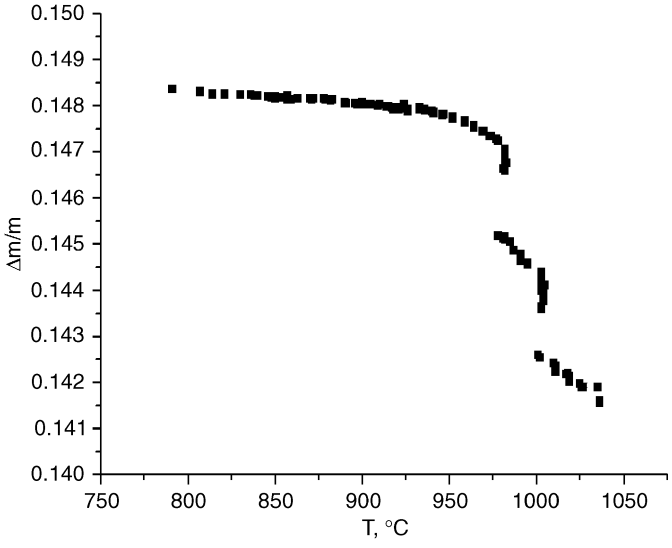

Fig. 1. Temperature dependence of weight changes for $LaNiO_{3-\delta}$ in air.

3.2. Determination of the stability limits for $LaNiO_{3-\delta}$, $La_3Ni_2O_{7-\delta}$ and $La_4Ni_3O_{10-\delta}$ by conductivity measurement method

Electrical conductivity of $LaNiO_{3-\delta}$, $La_3Ni_2O_{7-\delta}$ and $La_4Ni_3O_{10-\delta}$ was measured in the temperature range of 300–1300 °C in steps of 50 °C in air. However, starting from the point where conductivity starts changing not monotonically, we continue measuring in steps of 10 °C. The values of conductivity versus temperature are shown in Fig. 2. It is easy to see that drastic drop of conductivity for $LaNiO_{3-\delta}$ takes place at temperature about ~980 °C. This value is in a good agreement with the value measured by TGA. It can be seen that drastic drop of conductivity for $La_3Ni_2O_{7-\delta}$ and $La_4Ni_3O_{10-\delta}$ are very close to each other and take place at temperature about ~1200 °C. These results coincide with those reported in [30].

3.3. Determination of stability limits for $La_3Ni_2O_7$ and $La_4Ni_3O_{10}$ by EMF-measurement method

Comparing the average oxidation state of Ni ions within the $La_{n+1}Ni_nO_{3n+1}$ series, one could suppose that the stability limit with regard to oxygen partial pressure should decrease in the following row: $LaNi^{3+}O_3$–$La_4(Ni^{2.67+})_3O_{10}$–$La_3(Ni^{2.5+})_2O_7$–$La_2Ni^{2+}O_4$, similarly as it was found earlier in La–Co–O system [32,33] (although $La_3Co_2O_7$ was not found in this system). Hence, decomposition reactions for $La_4Ni_3O_{10}$ and $La_3Ni_2O_7$ can be represented in terms of reactions (3) and (4).

However, according to the results of X-ray powder diffraction, phases $La_4Ni_3O_{10}$, La_2NiO_4 and NiO were found after decomposition of $La_4Ni_3O_{10}$ in the first cell and there were $La_3Ni_2O_7$, La_2NiO_4, $La_4Ni_3O_{10}$ and NiO found in the second cell resulted from the decomposition of $La_3Ni_2O_7$. These results contradicted to the suggested

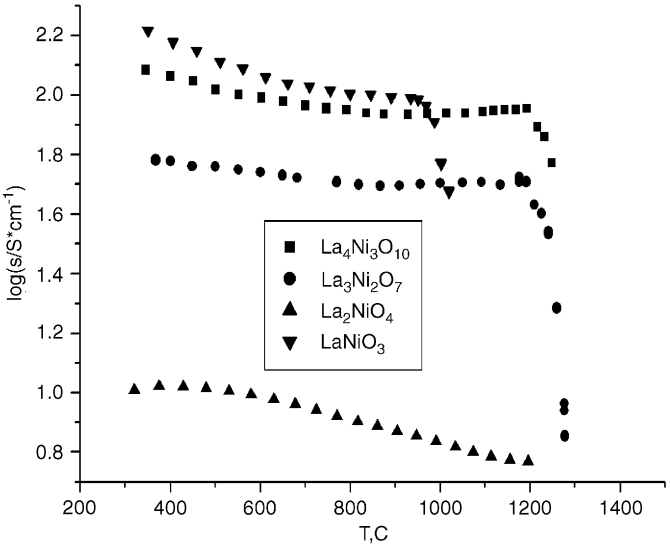

Fig. 2. Specific conductivity of the lanthanum nickelates as a function of temperature in air.

reactions (3) and (4). Moreover, in terms of the Gibb's phase rule, a number of coexisted phases in the second cell are more than maximum possible.

Let us suppose that the decomposition mechanism corresponded to the reactions (3) and (4), and the values of decomposition limits of $La_4Ni_3O_{10}$ and $La_3Ni_2O_7$ are very close to each other as it was presented in [31]. Then during the process of electrochemical oxygen removal, we could exceed decomposition limits of both $La_4Ni_3O_{10}$ and $La_3Ni_2O_7$, so that $La_3Ni_2O_7$ resulted from the decomposition of $La_4Ni_3O_{10}$ had started to transform into La_2NiO_4. This would lead to the appearance of four phases in the first cell. As for the second cell, decomposition of $La_3Ni_2O_7$ would result in the formation of La_2NiO_4 and NiO. These assumptions are in conflict with obtained experimental results.

Taking into account the phase composition of each cell, it is possible to assume another mechanism of decomposition processes. Let us suppose that $La_4Ni_3O_{10}$ is more stable in comparison with $La_3Ni_2O_7$; consequently, the reaction for the second cell can be written as follows:

$$\text{Cell 2}: \ 2La_3Ni_2O_{7-\delta} \rightarrow La_4Ni_3O_{10-\delta'} + La_2NiO_{4+\delta''} + (2\delta - \delta' + \delta'')/2O_2 \quad (6)$$

and

$$\text{Cell 1}: \ La_4Ni_3O_{10} \rightarrow 2La_2NiO_4 + NiO + \tfrac{1}{2}O2. \quad (7)$$

For the sake of simplicity, oxygen nonstoichiometry was not taken into account in reaction (7).

If decomposition limits of $La_4Ni_3O_{10}$ and $La_3Ni_2O_7$ are close to each other, then during the process of pumping oxygen out of the second cell, we could reach the pressure lower than the value of stability limit for both $La_3Ni_2O_{7-\delta}$ and $La_4Ni_3O_{10-\delta}$, which would lead to decomposition of $La_4Ni_3O_{10-\delta}$ in accordance with reaction (7) giving rise to additional product NiO.

Temperature dependences of EMF for both cells are represented in Fig. 3. It is obvious that experimental data for cells 1 and 2 nicely fitted as same linear dependence. This fact and suggested decomposition mechanism according the reactions (6) and (7) can lead to the conclusion that same equilibrium reaction, described by Eq. (7), had been measured in both cells. Small amount of oxygen, which acts in reaction (6), comes out from the difference in possible oxygen nonstoichiometry of coexisted phases, can hardly be enough for EMF technique use. The values of oxygen nonstoichiometry for the complex oxides in the reaction (6), calculated by the extrapolation of dependences obtained in [12] and in present work, show that the amount of oxygen in this reaction tends to zero. That is why we could not fix the equilibrium state corresponding to reaction (6) and skipped over to the equilibrium corresponding to reaction (7) in EMF experiment. This was the reason for coexistence of all four substances in the second cell when the experiment had been finished.

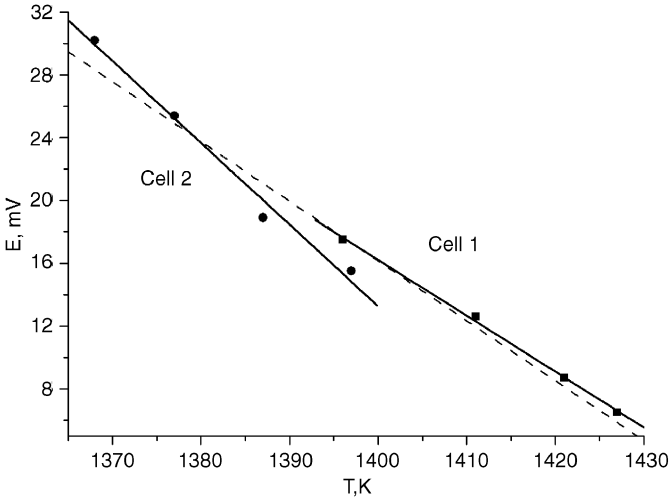

Fig. 3. Temperature dependence of EMF for the cells 1 and 2. Dash line—linear fitting of all experimental points together. Solid lines—linear fitting of experimental points of cells 1 and 2 separately.

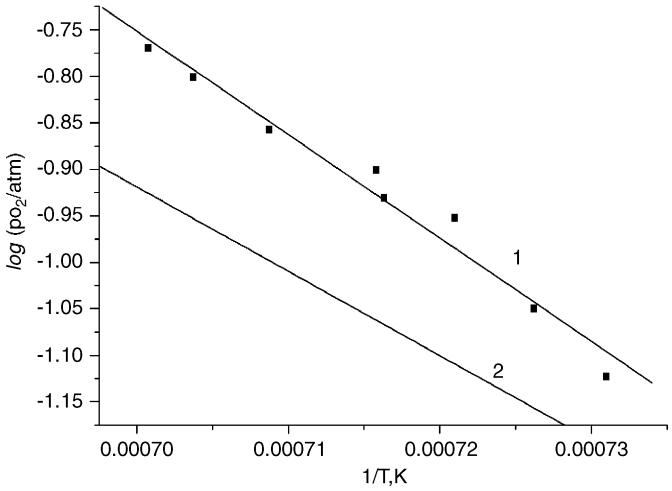

Fig. 4. Equilibrium oxygen pressure, corresponding to reaction (7) versus reverse temperature. (1) Measured points and linear regression obtained in the present work. (2) Dependence reported by us earlier [6,32].

In order to exclude errors connecting with the presence of additional phase, only experimental data obtained in the EMF measurements for the cell (1) were fitted by linear regression of four points as follows:

$$E(\text{mV}) = 514.6 - 0.356T(K)\ (\pm 0.8\,\text{mV}) \times (1396 \leqslant T, K \leqslant 1427). \quad (8)$$

Extrapolation of the linear dependence to $E = 0$ gives $T = 1173\,^{\circ}\text{C}$ which corresponds to decomposition temperature of $La_4Ni_3O_{10}$ in air. Taking into account narrow temperature range of EMF measurements, this value is sufficiently close to the approximate value determined by conductivity method (1200 °C). Eq. (8) can be easily transformed to the temperature dependence of equilibrium oxygen pressure, corresponding to reaction (7):

$$\log(PO_2/\text{atm}) = 6.50 - 10375.(1/T)\ (\pm 0.01). \quad (9)$$

Equilibrium oxygen pressure, corresponding to reaction (7), as a function of temperature is shown in Fig. 4. The differences between equilibrium pressures measured in the present work and values obtained in our laboratory earlier [6,32] consist $\Delta P = 0.02$ atm for the lowest temperature (1368 K) and $\Delta P = 0.06$ atm for the highest temperature (1427 K) (Fig. 4).

Temperature dependence of free Gibbs energy for reaction (7) was also calculated:

$$\Delta G^{\circ}(\mathrm{J}) = 99300 - 62.18T\ (\pm 200\ \mathrm{J}). \quad (10)$$

3.4. Oxygen nonstoichiometry of $La_3Ni_2O_{7-\delta}$ and $La_4Ni_3O_{10-}$

Absolute values of oxygen nonstoichiometry for $La_3Ni_2O_{7-\delta}$ and $La_4Ni_3O_{10-\delta}$ calculated from the mass changes during samples reduction in the flow of hydrogen at 1100 °C and 0.21 atm were found to be 0.068 and 0.165, respectively. Oxygen content found in $La_3Ni_2O_{6.932}$ is very close to that reported by Zhang et al. [16]. Temperature dependences of oxygen nonstoichiometry in air are shown in Fig. 5. The values of oxygen nonstoichiometry versus oxygen pressure at 1100 °C are shown in Fig. 6.

As consistent with electroneutrality condition, appearance of positively charged oxygen vacancies ($V_O^{\bullet\bullet}$) have to accompany the decrease of mean oxidation state of nickel ions. Calculated values of mean oxidation state of nickel ions in $La_3Ni_2O_{7-\delta}$ and $La_4Ni_3O_{10-\delta}$ versus temperature in air and versus PO_2 at 1100 °C are shown in Figs. 7 and 8, respectively. It is interesting to note that the difference between the values of mean oxidation state of Ni ions in $La_3Ni_2O_{7-\delta}$ and $La_4Ni_3O_{10-\delta}$ become smaller while the temperature increases and oxygen pressure decreases. At decomposition conditions determined in this work, at about 1200 °C in air or at $PO_2 \approx 10^{-1}$ atm at 1100 °C, this difference is about the same value 0.1. However, mean

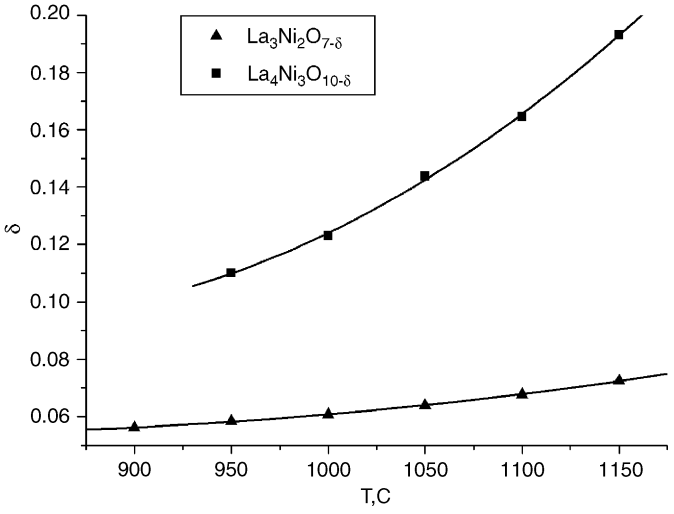

Fig. 5. Temperature dependences of oxygen nonstoichiometry for $La_3Ni_2O_{7-\delta}$ and $La_4Ni_3O_{10-\delta}$ in air.

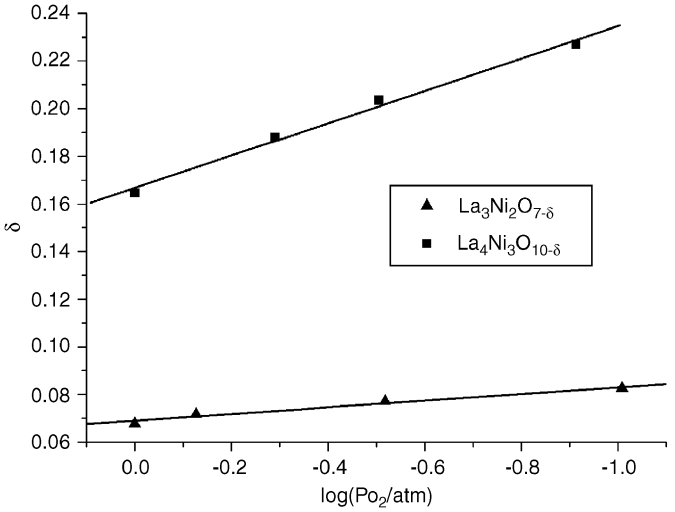

Fig. 6. Oxygen nonstoichiometry of $La_3Ni_2O_{7-\delta}$ and $La_4Ni_3O_{10-\delta}$ at 1100 °C as a function of oxygen partial pressure.

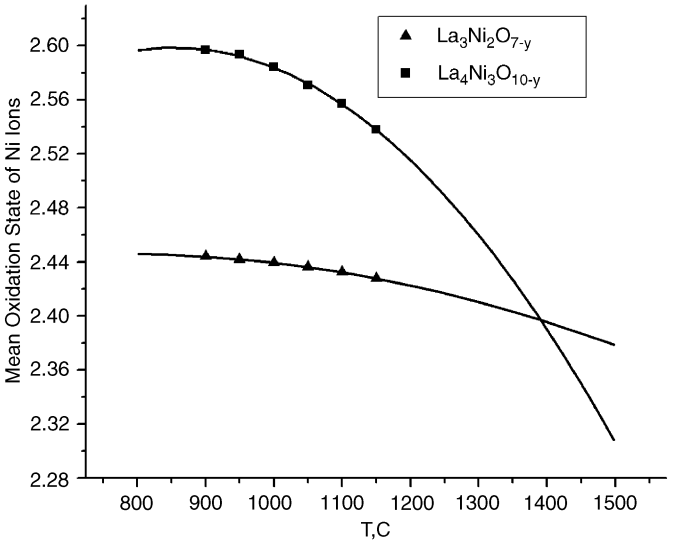

Fig. 7. Mean oxidation state of Ni ions in $La_3Ni_2O_{7-\delta}$ and $La_4Ni_3O_{10-\delta}$ versus temperature in air.

oxidation state of Ni ions in $La_3Ni_2O_{7-\delta}$ even at decomposition conditions is still smaller than those in $La_4Ni_3O_{10-\delta}$. In order to estimate thermodynamic parameters (T, PO_2) where the average oxidation state of Ni in $La_3Ni_2O_{7-\delta}$ and $La_4Ni_3O_{10-\delta}$ is getting equal, temperature and PO_2 dependences of the mean oxidation state of Ni,ions were fitted by polynomial and linear regressions, respectively. It was shown (Figs. 7 and 8) that cross points located behind decomposition conditions in both cases.

From the structural point of view, it should be mentioned that in $La_3Ni_2O_{7-\delta}$, nickel ions distributed over one type of crystallographic position, while in $La_4Ni_3O_{10-\delta}$, there are two different types of Ni sites [7]. From the precise structural study of $La_4Ni_3O_{10-\delta}$, it was suggested that Ni ions inside the oxygen octahedron, which located between perovskite layers and Ni ions inside the

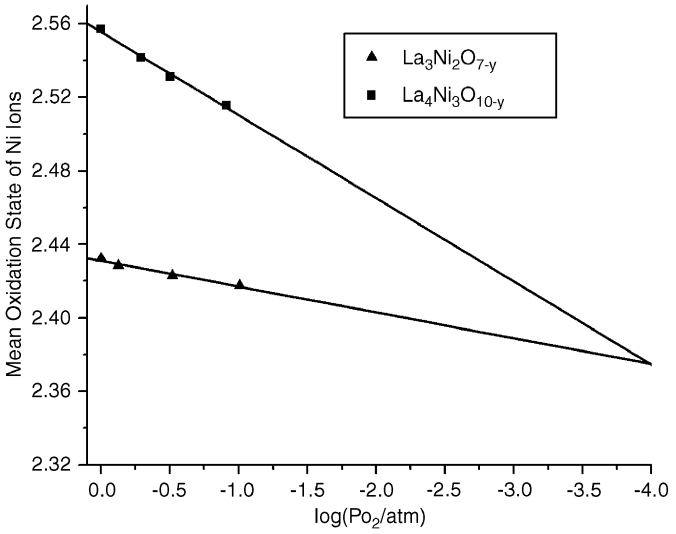

Fig. 8. Mean oxidation state of Ni ions in $La_3Ni_2O_{7-\delta}$ and $La_4Ni_3O_{10-\delta}$ as a function of oxygen pressure at 1100 °C.

oxygen octahedron, which adjoin to RS layers charged differently. Ni ions inside the oxygen octahedron, which located between perovskite layers, have higher oxidation state. Therefore, Ni ions in $La_4Ni_3O_{10-\delta}$ inside the oxygen octahedron, which adjoin to RS layers, have probably approximately same oxidation state or even lower as Ni ions in $La_3Ni_2O_{7-\delta}$. Also if the process of decomposition occurs by means of Ni ions diffusion, then in $La_3Ni_2O_{7-\delta}$, such jump through the RS layer can lead to the formation of three perovskite layers from the one side of RS (that corresponds to $La_4Ni_3O_{10}$ structure) and one perovskite layer left from the other side (corresponding to La_2NiO_4). Undoubtedly, suggested description of the disproportionate process is rather simplified but can be taken into account as a possible mechanism, which should be additionally confirmed.

3.5. Phase diagram of the La–Ni–O system

Since nickel ions possess different oxidation states in binary and all ternary oxides formed in the La–Ni–O system, it is impossible to represent all of them in one plane cross-section of phase diagram with variable oxygen pressure. However, in order to show all coexisted oxides in such type of systems, one can use the compositional axes, which takes into account relative mole fraction of metals. This method was successfully used earlier [6,31–33]. In fact, such kind of representation is the projection of three-dimensional phase diagram of the La–Ni–O system to the "La–Ni composition" versus oxygen pressure plane. Based on the conclusions made in this work, such isothermal (1400 K) projection of La–Ni–O system phase diagram was constructed (Fig. 9). The composition in the diagram was presented in terms of relative mole fractions of metallic components. Oxygen content in condensed phases is written as it is required for each particular formula. Since we have not determined limiting oxygen

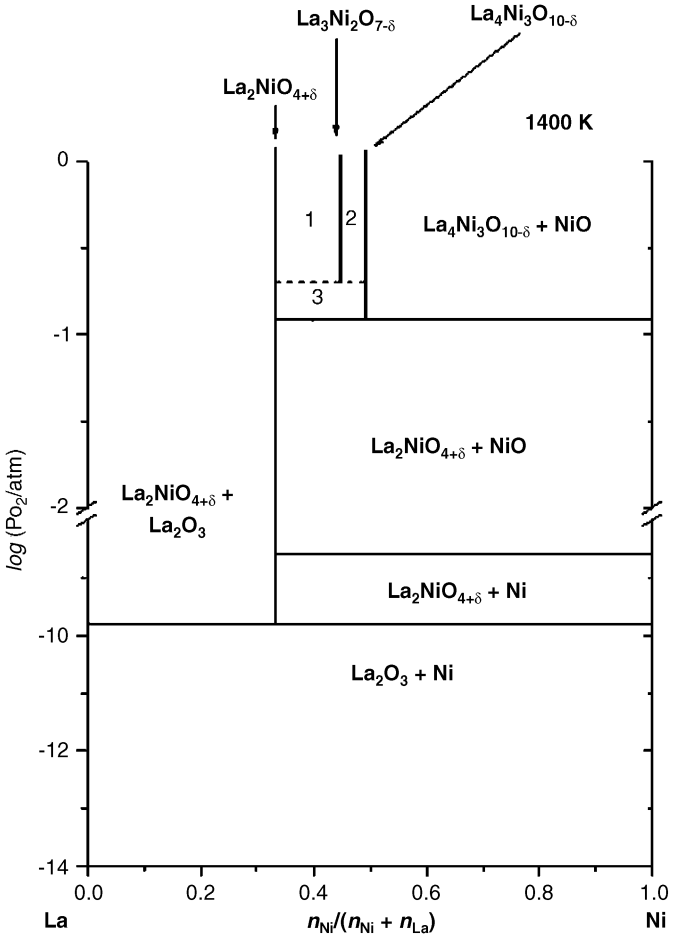

Fig. 9. Isothermal (1400 K) projection of La–Ni–O system phase diagram to the La–Ni mole fraction versus oxygen pressure plane. (1) $La_2NiO_{4+\delta}+La_3Ni_2O_{7-\delta}$, (2) $La_3Ni_2O_{7-\delta}+La_4Ni_3O_{10-\delta}$, (3) $La_2NiO_{4+\delta}+La_4Ni_3O_{10-\delta}$.

pressure for $La_3Ni_2O_{7-\delta}$ disproportionation, it is shown as the dotted line. Stability ranges of La_2NiO_4 and NiO have been taken from [6,32]. Phase boundaries obtained for $La_3Ni_2O_{7-\delta}$ and $La_4Ni_3O_{10-\delta}$ in the present study are close to those reported by Zinkevich and Aldinger [31], but the consequence of phase transformations is different.

4. Conclusion

Four single-phase samples members of homologous series $La_{n+1}Ni_nO_{3n+1}$ ($La_2NiO_{4+\delta}$, $La_3Ni_2O_{7-\delta}$, $La_4Ni_3O_{10-\delta}$ and $LaNiO_{3-\delta}$) have been prepared by the citrate technique. The stability limit of $LaNiO_{3-\delta}$ in air has been determined by conductivity measurements and thermogravimetric analysis. Decomposition temperatures of $La_3Ni_2O_{7-\delta}$ and $La_4Ni_3O_{10-\delta}$ in air have been determined by conductivity measurements. Alternative mechanism of $La_3Ni_2O_{7-\delta}$ decomposition was proposed. The stability limit of $La_4Ni_3O_{10-\delta}$ has been determined by means of EMF technique. Oxygen nonstoichiometry of $La_3Ni_2O_{7-\delta}$ and $La_4Ni_3O_{10-\delta}$ as a function of temperature and oxygen partial pressure has been measured by

thermogravimetric technique. On the basis of proposed decomposition processes for complex oxides, the projection of three-dimensional phase diagram of the La–Ni–O system to the La–Ni versus oxygen pressure plane at 1400 K was constructed.

Acknowledgments

This work was supported partly by grants from the Russian Foundation for Basic Researches (RFBR) N 05-03-32477 and (RFBR-Urals) N 04-03-96136, Program of Federal Agency of Science and Innovations of Russian Federation N 2006-PU-19.0/001/475.

References

[1] A. Rabenau, P. Eckerling, Acta Crystallogr. 11 (1958) 304–306.
[2] L.M. Golub, L.S. Sidorik, S.A. Nedilko, T.I. Fedoruk, Inorg. Mater. 14 (1978) 1866–1869 (in Russian).
[3] S.A. Nedilko, R.D. Vasyagina, L.S. Sidorik, M.N. Ermakova, S.M. Gogzinskii, Chem. J. Ukraina 46 (1980) 251–253 (in Russian).
[4] M.V. Kniga, R.A. Zareckaya, Inorg. Mater. 7 (1971) 464–467 (in Russian).
[5] V.F. Savchenko, Inorg. Mater. 17 (1981) 1654–1657 (in Russian).
[6] V.A. Cherepanov, A.N. Petrov, L.Yu. Grimova, E.M. Novickii, Russ. J. Phys. chem. 57 (1983) 859–863 (in Russian).
[7] V.I. Voronin, I.F. Berger, V.A. Cherepanov, L.Ya. Gavrilova, A.N. Petrov, A.I. Ancharov, B.P. Tolochko, S.G. Nikitenko, Nucl. Instrum. Methods Phys. Res. A 470 (2001) 202–209.
[8] A. Mehta, P.S. Heaney, Phys. Rev. B: Condens. Matter 49 (1994) 563–571.
[9] A. Demourgues, A. Wattiaux, J.C. Grenier, M. Pouchard, J.L. Soubeyroux, J.M. Dance, P. Hagenmuller, J. Solid State Chem. 105 (1993) 458–468.
[10] A. Demourgues, F. Weill, B. Darriet, A. Wattiaux, J.C. Grenier, P. Gravereau, M. Pouchard, J. Solid State Chem. 106 (1993) 317–329.
[11] D.E. Rice, D.J. Buttrey, J. Solid State Chem. 105 (1993) 197–210.
[12] E.N. Naumovich, M.V. Patrakeev, V.V. Kharton, A.A. Yaremchenko, D.I. Logvinovich, F.M.B. Marques, Solid State Sci. 7 (2005) 1353–1362.
[13] J.A. Kilner, C.K.M. Shaw, Solid State Ion. 154–155 (2002) 523.
[14] J.P. Tang, R.I. Dass, A. Manthiran, Mater. Res. Bull. 35 (2000) 411.
[15] J. Drennan, C.P. Tavares, B.C.H. Steele, Mater. Res. Bull. 17 (1982) 621–626.
[16] Z. Zhang, M. Greenblatt, J.B. Goodenough, J. Solid State Chem. 108 (1994) 402–409.
[17] M.D. Carvalho, F.M.A. Costa, I.S. Pereira, A. Wattiaux, J.M. Bassat, J.C. Grenier, M. Pouchard, J. Mater Chem. 7 (1997) 2107–2111.
[18] C.D. Ling, D.N. Argyriou, G. Wu, J.J. Neumeier, J. Solid State Chem. 152 (1999) 517–527.
[19] A.K. Tkalich, V.P. Glazkov, V.A. Somenkov, S.Sh. Shiljshtein, A.E. Karkin, A.V. Mirmeljshtein, Supercond.: Phys. Chem. Technol. 4 (1991) 2380–2385 (in Russian).
[20] M. Seppanen, Scand. J. Metall. 8 (1979) 191–192.
[21] Z. Zhang, M. Greenblatt, J. Solid State Chem. 117 (1995) 236–246.
[22] V.F. Savchenko, L.S. Ivashkevich, I.Ya. Lyubkina, J. Inorg. Chem. 336 (1988) 30–33 (in Russian).
[23] A. Wold, B. Post, E. Banks, J. Am. Chem. Soc. 79 (1957) 4911–4913.
[24] G. Demazeau, A. Marbeuf, M. Pouchard, P. Hagenmuller, J. Solid State Chem. 3 (1971) 582–589.
[25] T. Nakamura, G. Petzov, L.I. Gauckler, Mater. Res. Bull. 14 (1979) 649–659.
[26] M. Crespin, P. Levitz, L. Gatineau, J. Chem. Faraday Trans. 79 (1983) 1181–1194.
[27] N.I. Timofeeva, I.V. Romanovich, Inorg. Mater. 7 (1971) 1878–1879.
[28] C. Brisi, M. Vallino, F. Abbattista, J. Less-Common Met. 79 (1981) 215–219.
[29] P. Odier, J.P. Bouraly, J.M. Plessier, Silic. Ind. 50 (1985) 17–24.
[30] P. Odier, Y. Nigara, J. Coutures., J. Solid State Chem. 56 (1985) 32–40.
[31] M. Zinkevich, F. Aldinger, J. Alloys Compd. 375 (2004) 147–161.
[32] A.N. Petrov, V.A. Cherepanov, A.Yu. Zuev, V.M. Zhukovsky, J. Solid State Chem. 77 (1988) 1–14.
[33] A.N. Petrov, V.A. Cherepanov, E.M. Novitsky, V.M. Zhukovsky, Russ. J. Phys. Chem. 58 (1984) 1618 (in Russian).